INFLUENCES ON VERTICAL SHALLOW CRUST DEFORMATIONS IN THE CARPATHIAN-DANUBIAN-PONTIC AREA, AN EARTH SCIENCE INTEGRATED THEMATIC SERVICE CASE STUDY

E.I. NASTASE [1], A. MUNTEAN[1], S. NISTOR[2], S. DIMITRIU[3], M.N. JECU[1], N.SZ. SUBA[2]

[1] National Institute for Earth Physics, PO BOX MG2, 077125, Magurele, Romania
E-mails: eduard_nastase@infp.ro, muntean@infp.ro, mihaela.nicoleta.jecu@gmail.com
[2] University of Oradea, Faculty of Construction, Cadastre and Architecture, Oradea, Romania,
E-mails: sonistor@uoradea.ro, nsuba@uoradea.ro
[3] TOPGeocart, Bucharest, Romania,
E-mail: sorin.dimitriu@topgeocart.ro

Received July 11, 2021

Abstract. We describe a comprehensive analysis of permanent Romanian *Global Navigation Satellite System* (GNSS) sites' on vertical position time series from data spanning 3–20 years. The GPS observations were computed using Gipsy X software, we apply *Global Positioning System* (GPS) Imaging, a new technique for robust estimation of the vertical velocity field of the Earth's surface, and the final estimates to obtain the stations' vertical deformations velocities were analyzed using *Maximum Likelihood Estimation* (MLE) and *Median Interannual Difference Adjusted for Skewness* (MIDAS) trend estimator which is insensitive to undocumented steps, outliers, seasonality, and heteroscedasticity. We focus on the known national GPS observation level model in the Carpathian-Danubian-Pontic area to advance geodetic observation precision/accuracy toward 0.1 mm/year and therefore further constrain models of GIA and subsequent present-day ice mass change estimates at 45 degrees latitudes. Finally, we interpolate the data using weighted median estimation on a grid. The resulting velocity field is temporally and spatially robust, and edges in the field remain sharp. Our investigation results into a case study and an integrated thematic service of influences that could be applied to the revised analysis strategies of vertical deformations over the Romanian region.

Key words: *Global Positioning System* (GPS); *Precise Point Positioning* (PPP); *Maximum Likelihood Estimation* (MLE); vertical land motion; Geodesy; *Median Interannual Difference Adjusted for Skewness* (MIDAS); GPS Imaging.

1. INTRODUCTION

The latest years reveal to us the necessity and the interest to develop an integrated research platform to improve skills in answering fundamental scientific questions in the field of Earth sciences and questions in the socio-economic field related to geo-hazards and geo-resources at the European level, a platform known by EPOS – *European Plate Observing System*.

Main objectives such as the implementation of thematic services (TCS) for different communities in EPOS, development of integrated services (ICS) for interoperability, data management and access to services, and ensuring the long-term financial and legal sustainability of EPOS – ERIC and implementing services leads to the harmonization of EPOS implementations with the national strategy. As a result, many European states mirror the EPOS platform at the national level and Romania is one of them (Integrated thematic services in the field Earth Observation – A national platform for innovation – SETTING).

A thematic core service for both EPOS and SETTING projects is the GNSS (*Global Navigation Satellite System*) Data and Products, and as a case study in the field of satellite geodesy, we analyzed the influences on vertical shallow crust deformations. Talking about geodesy, this is the science of computing both the size and shape of our planet. In addition, it also refers to the computation and distribution analysis of the globe's gravitational field. It also relates to geodetic astronomy, which is oriented towards defining, shaping, and computing reference frameworks of terrestrial (and celestial) type. It involves various space observation methods.

The vertical motion of the Earth's crust is affected by many processes [1]. The well-known *glacial isostatic adjustment* (GIA) is the process with the most significant impact on the global sea level and it is followed by the loss of the continental ice sheets, which has horizontal wavelengths of 1000s of km [2, 3]. However, many other processes contribute to vertical shallow crust deformations in a variety of rates, patterns, and wavelengths. With the help of GNSS *Continuous Operating Reference Station* (CORS), we can study those processes that include tectonic uplift, sea-level variation [4, 5], water vapor determination [6–9], ocean-tide measurements [10], earthquake (cycle deformation) and tsunami monitoring [11], sediment loading [12], and geodynamics applications that study changes in mantle flow or dynamic topography [13–18, 19]. Short-term factors such as changes in the terrestrial hydrosphere and climate lead to unsteady vertical deformations in cases of elastic response to contemporary ice loss [20, 21] or sediment compaction [22].

Human activity can also affect and trigger these processes [23, 24].

2. METHODS

We present an analysis of a national ~ 50 GNSS CORS [25] (part of EPOS and SETTING, see Fig. 1) and an extensive database of GPS data from NGL (http://geodesy.unr.edu/NGLStationPages/gpsnetmap/GPSNetMap.html).

The data processing was performed with Gipsy X software [26] using *precise point positioning* strategy (PPP). Gipsy X is a post-processing software developed at NASA's *Jet Propulsion Laboratory* (JPL), Pasadena USA. The idea behind PPP

is that the best available models and post-processed data are used to obtain very precise daily solutions for the network's GNSS stations.

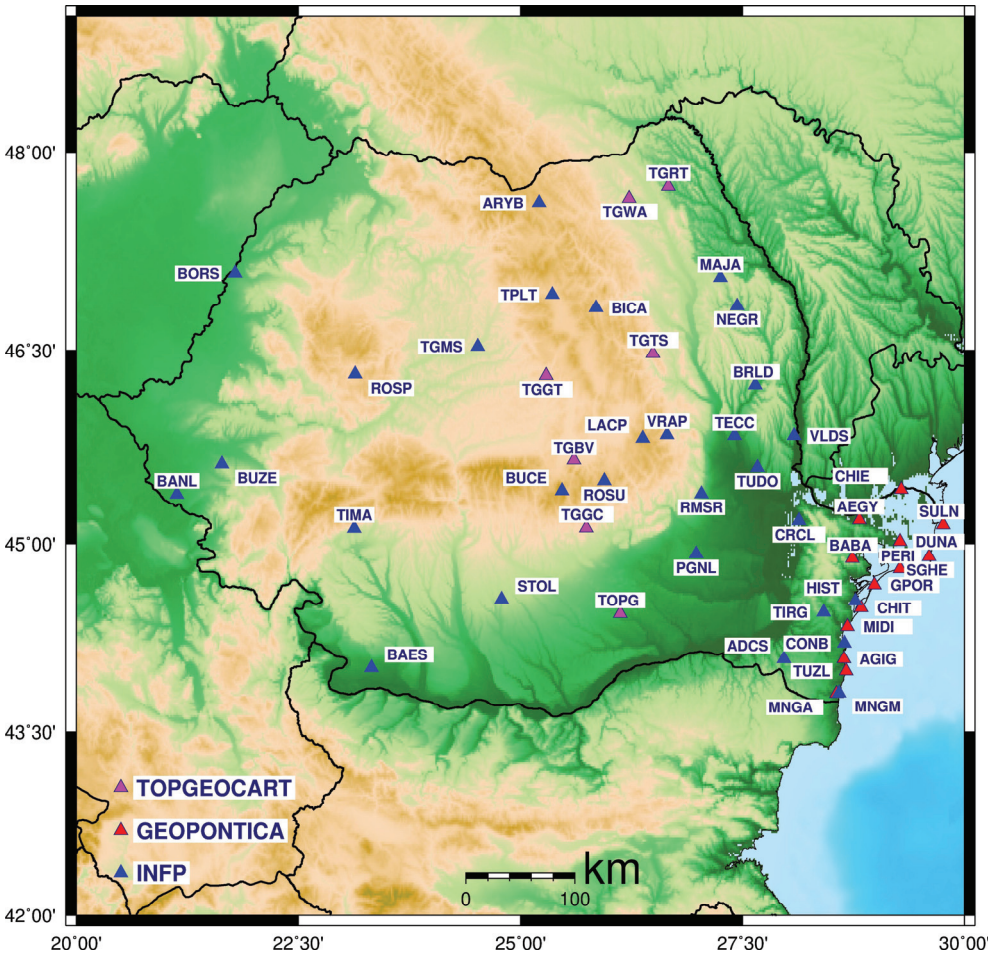

Fig. 1 – EPOS and SETTING GNSS Stations in Romania.

Models for wet atmospheric distortion [27], ocean loading displacement [28] of the site are used to correct all the effects that can influence the results. Accurate GNSS satellite orbits and clocks are obtained from JPL, every set of products contains files with consistent orbital state estimates, transmitter clock estimates, space-craft attitude information, *Earth rotation parameter* (ERP) estimates and widelane phase biases information.

The results are so-called non-fiducial position solutions, these position solutions are then transformed into the last International Terrestrial Reference Frame, using a global 7 Helmert parameter (3 small rotations, 3 translations, 1 scale parameters)

transformation also provided by JPL. The daily ITRF solutions are converted to a reference tectonic plate, the fixed Eurasian plate, using the most recently published rotation pole solution of that plate in the ITRF14 reference frame [29].

The Earth behaves under various loads, provides information about the source and magnitude of forcings; the analysis reveals the measurement of these motions and can be used to estimate the Earth's material and rheological properties.

We will now focus on a new analysis method called GPS Imaging, that uses robust and unbiased estimation to deal with noise and uncertainty to enhance the signals of flex and flow in the solid Earth. This result is a stable interpolation of the data, leading to better visualization and interpretation, with greater impact and utility for geodynamic investigations. The velocities obtained with the recently developed non-parametric MIDAS algorithm [30] on the IGS14-aligned time series that reduces the impact of seasonality, undocumented steps, and outliers in the position time series were used as input. The method is robust in the sense that the final result is insensitive to outliers up to a breakdown point (up to 25% incorrect data).

To determine the seasonal signal and at the same time to do a noise analysis which measures the amount of white noise and power law – flicker and random walk noise in the time series – we used *maximum likelihood estimation* (MLE) as described by [31–35]. MLE is also used to establish an overall power law noise model that best describes the data. The probability function is maximized to estimate the noise component using MLE, by adjusting the data covariance matrix. Therefore:

$$l(x,C) = \frac{1}{(2\pi)^{\frac{N}{2}} (detC)^{\frac{1}{2}}} \exp(-0.5\hat{v}^T C^{-1}\hat{v}) \tag{1}$$

where:

- l is the likelihood
- *det* represents the determinant of the matrix,
- C represents the covariance matrix of the assumed noise in the data
- N is the number of epochs end
- $\hat{v}$ is the post-fit residuals of the linear function using weighted least squares with the same covariance matrix C.

In terms of stability the logarithm of the likelihood has to be maximized or minimize the negative:

$$MLE = \ln[l(x,C)] = \frac{1}{2}[\ln(\det C) + \hat{v}^T C^{-1}\hat{v} + N\ln(2\pi)] \tag{2}$$

due to the fact that the maximum is unaffected by the monotonic transformations.

The typical model is composed by an intercept, a linear trend (velocity), sinusoidal terms represented by annual and semiannual signal, terms for offsets and in the case of a large coseismic event, a term to describe the postseismic motion [36]. The covariance matrix C can correspond to different stochastic noise such as white, power law, moving average, autoregressive, first-order Gauss Markov, band pass and also combination between these different types of noise. If it is assumed that we are dealing with a white noise component and power law then the matrix is:

$$C = a_w^2 I + b_k^2 J_k \tag{3}$$

where a_w and b_k represent the white respectively the power law noise amplitudes, I is the $n \times n$ identity matrix and J_k is the power law covariance matrix with spectral index k. Although the equation (3) presents only two types of noise, the time series may contain more than these two types of noise and sometimes may not be power law noise [36].

By fitting a straight line through a series of n points x_i taken at time t_i which represents the basic liner regression problem, the determination of rate uncertainties is given by:

$$x_i = x_0 + rt_i + \varepsilon_x(t_i) \tag{4}$$

where $\varepsilon_x(t_i)$ represents the error term.

Assuming that $\varepsilon_x(t_i)$ is subjected to linear combination of independent random variables and it is identically distributed, $\alpha(t_i)$, and a sequence of temporally correlated random variables, $\beta(t_i)$ such as:

$$\varepsilon_x(t_i) = \alpha\,\alpha(t_i) + b_k\beta(t_i) \tag{5}$$

the amplitude of white noise is represented by the scalar factor a and $b_{k\neq 0}$ is the scale factor of colored noise of spectral index k.

3. RESULTS

Based on the Bian *et al.* 2020 [37] study of the vertical deformation of the hydrological load at IGS stations over Europe, where GRACE was used to monitor the influence of the hydrological load on the non-linear motion of GPS stations and in terms of results of influences of GIA [3], seasonality (hydrological loading), and noise, possible groundwater variations were used the results for Tables 1 and 2 with the newest references (analysis).

Table 1

Statistics of uncertainties of the velocity in mm/year [36]

Statistics	Flicker			Powerlaw			MIDAS		
	East	North	Up	East	North	Up	East	North	Up
Min	0.046	0.045	0.159	0.026	0.036	0.073	0.115	0.110	0.444
Max	0.502	0.463	1.399	0.282	0.415	1.289	0.619	0.410	1.835
1st quertile	0.088	0.085	0.305	0.069	0.073	0.208	0.163	0.163	0.582
Median	0.114	0.108	0.393	0.092	0.092	0.282	0.182	0.188	0.681
3rd quertile	0.159	0.152	0.568	0.124	0.117	0.410	0.225	0.224	0.827

Table 2

Vertical volume flux rate of Earth's major land masses [39]

		Flux GPS Imaging			Flux GIA Model ICE-6G			Residual (non-GIA VLM)		
		Total	Positive	Negative	Total	Positive	Negative	Total	Positive	Negative
Land Mass	**Percent of Total**	(km^3/yr)			(km^3/yr)			(km^3/yr)		
Eurasia	9.88%	5.1	18.8	–13.8	22.2	22.9	–0.7	–17.1	–4.0	–13.1

In the study were not taken into consideration time series shorter than 3.5 years and mean completeness (number of observation days per year divided by 365 days) of less than 30% following the same criteria as [39]. Those stations were omitted because they offer less constraint on vertical deformations, but for favorable picture of the spatial distribution of stations, we keep them on the Fig. 1. After these exclusions, 95% of the stations have completeness greater than 86%. The median/maximum time series duration is 6.4/19.1 years, 85% have their first position on or after the year 2013.0. All the statistics presented above were applied only to the ~ 50 GNSS CORS part of EPOS and SETTING.

In cases where stations aren't collocated, Delaunay triangulation of the network works best for GPS Imaging. Therefore, before imaging, we decluster the stations, creating single representative meta-stations with a vertical rate that is the weighted median value in the cluster when stations are within 0.1 km of one another. The uncertainty of the cluster rate is determined as if it were a weighed mean of the contributing rates, where the weights are one over the uncertainties, making large uncertainty rates unlikely to contribute [38, 39] see Fig. 2.

In the development of the SETTING platform services, the main object was to build an efficient, complete and multidisciplinary research platform in the field of Earth Sciences in Romania.

In addition, there was a desire to have modules implemented with a statistical profile in order to offer the administration staff a clear vision related to the activities performed by the station and easy access to the information for the users.

The software development process is represented by a structure applied to the development of a software product. In this situation, the model naming to develop the software solution is a waterfall.

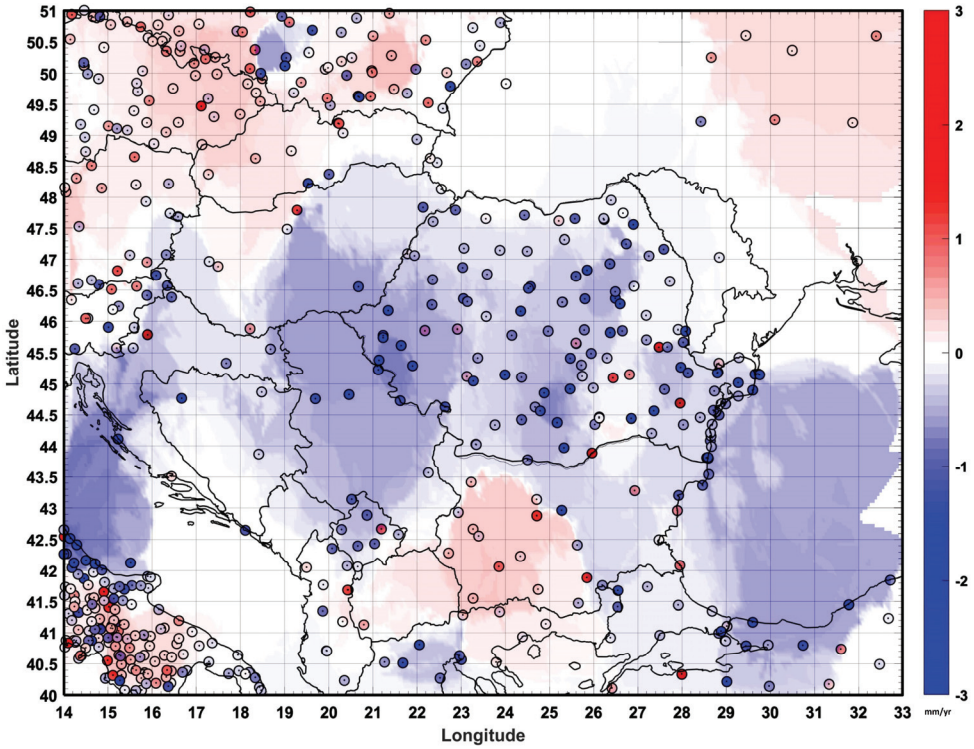

Fig. 2 – (Color online) MIDAS vertical GPS velocities for Romania in a regional context, for all stations with over 2.5-year time series duration, in the IGS14 reference frame. The color scale is in mm/yr; positive (red) is upward, and negative (blue) is downward.

Technically speaking, GNSS services was developed by joining two development environments (Frontend and Backend) plus a second app who is totally independent. The purpose of the last enounced is to manage the database. All of them are running on different ports. The necessary configurations for establishing the connection are made on host server. The backend was developed in Java (Spring framework [40]) and Frontend through the medium of Angular Framework [41] and also Bootstrap, PimeNG, Chart.js libraries (the last one was used for graphical representations). GNSS offers crud operations (create, read, update, delete), the reason why a mysql database was implemented. Database serves information to user through functions implemented in backend section.

Even if it is a standalone application, GNSS becomes a module for SETTING's platform. The main sections have a statistical role (rendering graphical representations based on input data set). It supposes dataset registration (into the database), analysis, processing, or data filtering.

These functionalities depend and are implemented on the application backend side after being taken and analyzed by the frontend.

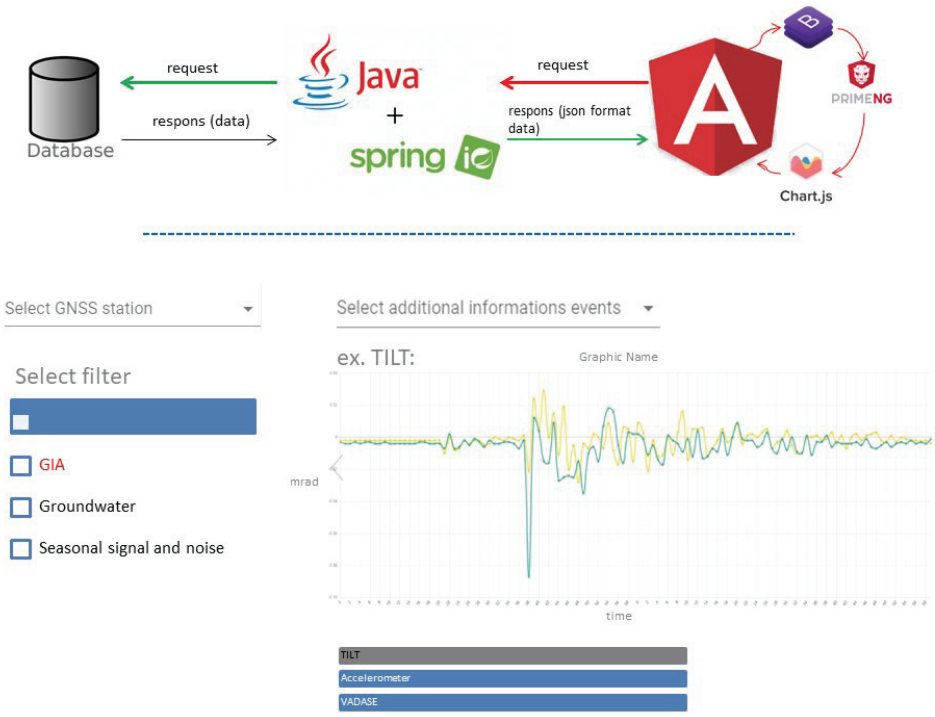

Fig. 3 – In the following, we can see the interaction between the technologies described above and the libraries used (bootstrap, primeng, chart.js) for a lineChart output. User Interface (Angular) makes a request to backend (JavaSpring), making another request to Database. The returned data arrives in backend and frontend at the last.

Depending on users' needs, data can be returned on different chart types (lineChart, barChart, pieChart, etc.). In our situation the relevant type of chart is the lineChart. This chart offers a detailed overview for data where *Ox* axis is destined for "DateTime" data type and *Oy* axis for numeric data type like "Double", "Float", "Integer" (we can mention the fact that on *Oy* axis multiple datasets can exist). See Fig. 3.

Each graphics library has its own type of data registrations. Chart.js [42] is a dedicated library for graphical representation. The received information in *json* format is parsed and returned as a friendly graph, easy to understand by users.

4. DISCUSSION AND CONCLUSION

The work performed is very important because we managed to create a unique GNSS database from a homogeneous combination of all permanent networks and to create metadata in a proper, international standard format for all stations. We think that it will be easier for future national and international projects to make a

research study having all these stations at our disposal to promote interdisciplinary interoperability**,** with a special focus on seismology and geology. With GNSS, we can study deformation associated with earthquakes. These measurements are complementary to seismological data because they document the full earthquake cycle, including interseismic and transient postseismic processes, as well as coseismic deformation.

Having now a dense and homogeneous permanent network will help us to understand the geodynamic processes that occurred at national level (Romania) and there is a clear need to think of an interpretation into a large geodynamics framework, looking at the larger interaction effects between the Pancardi system, the southeastern East European and Scythian Platform, the Aegean System and all the way south to the North African Domain.

EPOS and SETTING projects aimed for integration of existing research infrastructures in Europe and at the national level in the field of Earth Sciences (data infrastructures and facilities) and so they build an efficient, complete and multidisciplinary research platform in the field, allowing access to data and products by establishing access policies.

An electronic research infrastructure was developed for data integration of products and services offered to users and contributed to building a community for Earth Sciences by promoting cooperation with complementary projects in geosciences (Geo, ICT, and environmental sciences) and offering services to different users and authorities.

Analyzing the non-GIA vertical deformations, a correlation is found between seasonality and uplift trends with observations from gravity data suggesting that the loading from the terrestrial hydrosphere is quite dominant.

Although stations are dominantly concentrated at subsiding parts of continents, GPS Imaging geographically balances VLM signals, correcting for bias associated with network distribution [39].

Part of the influences study analysis considered the GNSS CORS network in Romania regarding the type of dominant noise, its related amplitude, and seasonal signal. Three types of noise combinations were used to evaluate the GNSS stations: FL + WN, PL + WN and RW + WN defined by Nistor *et al.* 2021 [36]. The dominant type of noise based on the analysis of the *MLL* revealed that in general, the FN + WN is the best noise model for all the analyzed stations. In the case that the PL + WN presented higher *MLL* when the spectral index was analysed, we found that it is ~1, which is an indicator of FN.

In terms of noise amplitude, we can observe that the TGRef GNSS network is the nosiest network compared to other GNSS networks from Romania, but its primary application is to provide real-time correction for surveyors to do cadastral measurements. Also, in the regions where we had stations from 2 CORS networks, such as Bihor County and in the coastal area of the Black Sea, we can observe that all the stations show similar patterns in terms of noise amplitude. Higher values are

seen in the TGRerf network in terms of seasonality, but this can be attributed to the type of moment used to place the GNSS antenna because even stations from different CORS networks show notable differences, especially for the Up component [36].

We took one step further by applying a filter to obtain an optimal combination of data from collocated high-rate GPS and very high-rate accelerometer stations, which takes advantage of the strengths and minimizes the weaknesses of both data types. This resulted in a new methodology for providing displacement time series with millimeter/centimeter precision that can be used to have a better assessment of the seismic source [25, 44].

Analyzing and filtering the global influences of GIA and in particular for the northern latitude of 45 degrees, the seasonal variations of each individual GNSS station, making associations and correlations between the activity and the overlap of the aquifer with the highest subduction values obtained, we can reach the most accurate values of vertical surface deformations of the Earth's crust in the Carpathian-Danubian-Pontic area.

According to Hammond *et al.* 2021 [39], the net vertical flux from GPS Imaging averaged over the continents indicates that the non-GIA sources have about 70% of the impact of GIA's contribution to vertical deformations. Comparison between GPS and GRACE data in his study [39] show that most trends, seasonal changes, and multi-annual variability in vertical deformations come from the interaction of Earth's surface with its fluid envelopes. Hydrological loading affects nearly all of Earth's surface.

Acknowledgements. This paper was carried out within project SETTING Integrated thematic services in the field of Earth observation – a national platform for innovation, cofounded from the *Regional Development European Fund* (FEDR) through the Operational Competitivity Programme 2014–2020, Contract No. 336/390012 and NUCLEU Program MULTIRISC, supported by MCI, project no PN19080201. The Gipsy X software is licensed to the Department of Geophysics of the University of Bucharest (UNIBUC). We (the National Institute of Earth Physics, NIEP) were allowed to use this software in an ongoing collaboration with UNIBUC.

REFERENCES

1. J. Pfeffer, G. Spada, A. Mémin, J-P. Boy, and P. Allemand, *Decoding the origins of vertical land motions observed today at coasts*, Geophys. J. Int. **210** (1), p. 148–165 (2017).
2. L. Caron, E.R. Ivins, E. Larour, S. Adhikari, J. Nilsson, and G. Blewitt, *GIA model statistics for GRACE hydrology, cryosphere, and ocean science*, Geophys. Res. Lett. **45**, 2203–2212 (2018).
3. Y. Sun and R. E. M. Riva: *A global semi-empirical GIA model based on GRACE data*, Earth Syst. Dynam. **11**, 129–137 (2020).
4. J.S. Löfgren and R. Haas, *Sea level measurements using multi-frequency GPS and GLONASS observations*, EURASIP Journal on Advances in Signal Processing 2014 (1), 1–13 (2014).
5. K.M. Larson, T. Lay, Y. Yamazaki, K.F. Cheung, L. Ye, S.D.P. Williams and J.L. Davis, *Dynamic Sea Level Variation From GNSS: Shumagin Earthquake Tsunami Resonance and Hurricane Laura*, Geophysical Research Letters **48** (4) (2020).
6. A.H. Dodson, P.J. Shardlow, L.C.M. Hubbard, G. Elgered and P.O.J. Jarlemark, *Wet tropospheric effects on precise relative GPS height determination*, Journal of Geodesy **70** (4), 188–202 (1996).

7. J. Douša, *The impact of errors in predicted GPS orbits on zenith troposphere delay estimation*, GPS Solutions **14** (3), 229–239 (2009).
8. S. Nistor and A.S. Buda, *Using different mapping function in GPS processing for remote sensing the atmosphere*, Journal of Applied Engineering Science **5** (2), 73–80 (2015).
9. S. Nistor and A.S. Buda, *Evaluation of the ambiguity resolution and data products from different analysis centers on zenith wet delay using PPP method*, Acta Geodynamica et Geomaterialia **14**, No. 2 (186) (2017).
10. M. King and S. Aoki, *Tidal observations on floating ice using a single GPS receiver,* Geophysical Research Letters **30** (3) (2003).
11. C. Shi, Y. Lou, H. Zhang, Q. Zhao, J. Geng, R. Wang, R. Fang and J. Liu, *Seismic deformation of the Mw 8.0 Wenchuan earthquake from high-rate GPS observations*, Advances in Space Research **46** (2), 228–235 (2010).
12. E.R. Ivins, R.K. Dokka and R.G. Blom, *Post-glacial sediment load and subsidence in coastal Louisiana*, Geophys. Res. Lett. **34**, L16303 (2007).
13. W.C. Hammond, *Northwest Basin and Range tectonic deformation observed with the Global Positioning System*, 1999–2003. Journal of Geophysical Research **110** (B10), B10405 (2005).
14. S.D.P. Williams and P. Willis, *Error Analysis of Weekly Station Coordinates in the DORIS Network*, Journal of Geodesy **80** (8), 525–539 (2006).
15. S. Nistor and A.S. Buda, *GPS network noise analysis: a case study of data collected over an 18-month period*, Journal of Spatial Science, 1–14 (2016a).
16. S. Nistor and A.S. Buda, *The influence of different types of noise on the velocity uncertainties in GPS time series analysis*, Acta Geodynamica et Geomaterialia **13** (4), 387–394 (2016b).
17. K. Maciuk and S. Szombara, *Annual crustal deformation based on GNSS observations between 1996 and 2016*, Arabian Journal of Geosciences **11** (21), 667 (2018).
18. E. Şengül-Uluocak, R.N. Pysklywec, O.H. Göğüş, and E.U. Ulugergerli, *Multidimensional geodynamic modeling in the Southeast Carpathians: Upper mantle flow- induced surface topography anomalies*, Geochemistry, Geophysics, Geosystems **20**, 3134–3149 (2019).
19. C. Kreemer, G. Blewitt and P. Davis, *Geodetic evidence for a buoyant mantle plume beneath the Eifel volcanic area, NW Europe*, Geophys. J. Int. **222** (2), p. 1316–1332 (2020).
20. C.F. Larsen, R.J. Motyka, J.T. Freymueller, K.A. Echelmeyer and E.R. Ivins, *Rapid viscoelastic uplift in southeast Alaska caused by post-Little Ice Age glacial retreat*, Earth Planet. Sci. Lett. **237**, 548–560 (2005).
21. F. Pintori, E. Serpelloni, L. Longuevergne, A. Garcia, L. Faenza, L. D'Alberto, *Mechanical response of shallow crust to groundwater storage variations: Inferences from deformation and seismic observations in the eastern Southern Alps, Italy*, Journal of Geophysical Research: Solid Earth **126** (2021).
22. K. Johnson, W.C. Hammond, R. Burgette, S.T. Marshall and C.C. Sorlien, *Present-day and long-term uplift across the Western Transverse Ranges of Southern California*, J. Geophys. Res. – Solid Earth **125**(8) (2020).
23. S. Hainzl, T. Kraft, J. Wassermann, H. Igel and E. Schmedes, *Evidence for rainfall-triggered earthquake activity*, Geophys. Res. Lett. **33**, L19303 (2006).
24. M. Sneed, J. Brandt and M. Solt, *Land subsidence along the Delta-Mendota Canal in the northern part of the San Joaquin Valley, California*, 2003–10: U.S. Geological Survey Scientific Investigations Report **87**, 2013–5142 (2013).
25. E. Nastase, A. Muntean, S. Nistor, B. Grecu, D. Tataru, *GPS processing tools for better impact assessment of earthquakes in Romania*, Romanian Reports in Physics **72**, 707 (2020).
26. Bertiger, W., Bar-Sever, Y., Dorsey, A., Haines, B., Harvey, N., Hemberger, D., Heflin, M., Lu, W., Miller, M., Moore, A.W., Murphy, D., Ries, P., Romans, L., Sibois, A., Sibthorpe, A., Szilagyi, B., Vallisneri, M., and Willis, P., *GipsyX/RTGx, a new tool set for space geodetic operations and research: Advances in Space Research* **66** (3), p. 469–489, doi:10.1016/j.asr.2020.04.015, (2020).
27. re3data.org: *VMF Data Server; editing status 2020-12-14*; re3data.org – Registry of Research Data Repositories. http://doi.org/10.17616/R3RD2H, (2020).

28. M.S. Bos, H.G. Scherneck, Chalmers University of Technology, *Ocean tide loading provider*, (2013).
29. Z. Altamimi, P. Rebischung, L. Métivier, X. Collilieux, *ITRF2014: a new release of the international terrestrial referenceframe modeling nonlinear station motions*, J. Geophys. Res.: SolidEarth **121** (8), 6109–6131 (2016).
30. G. Blewitt, C. Kreemer, W.C. Hammond and J. Gazeaux, *MIDAS trend estimator for accurate GPS station velocities without step detection*, J. Geophys. Res. – Solid Earth **121**, 2054–2068 (2016).
31. J. Langbein and H. Johnson, *Correlated errors in geodetic time series: Implications for time-dependent deformation,* Journal of Geophysical Research: Solid Earth **102** (B1), 591–603 (1997).
32. J. Zhang, Y. Bock, H. Johnson, P. Fang, S. Williams, J. Genrich, S. Wdowinski and J. Behr, *Southern California permanent GPS geodetic array: Error analysis of daily position estimates and site velocities*, Journal of Geophysical Research: Solid Earth **102** (B8), 18035–18055 (1997).
33. M.S. Bos, R.M.S. Fernandes, S.D.P. Williams and L. Bastos, *Fast error analysis of continuous GPS observations*, Journal of Geodesy **82** (3), 157–166 (2008).
34. M.S. Bos, R.M.S. Fernandes, S.D.P. Williams and L. Bastos, *Fast error analysis of continuous GNSS observations with missing data*. Journal of Geodesy **87** (4), 351–360 (2013).
35. S.D.P. Williams, *CATS: GPS coordinate time series analysis software*, GPS solutions, **12** (2), 147–153 (2008).
36. S. Nistor, N.S. Suba, K. Maciuk, J. Kudrys, E.I. Nastase, A. Muntean, *Analysis of Noise and Velocity in GNSS EPN-Repro 2 Time Series*, Remote Sens. **13**, 2783 (2021).
37. Y. Bian, J. Yue, Z. Li, K. Cong, W. Li, Y. Xing, *Comparisons of GRACE and GLDAS derived hydrological loading and the impacts on the GPS time series in Europe*, Acta Geodyn. Geomater. 17, No. **2** (198), 297–310 (2020).
38. W.C. Hammond, G. Blewitt and C. Kreemer, *GPS Imaging of vertical land motion in California and Nevada: Implications for Sierra Nevada uplift*, J. Geophys. Res. 121, n. 10, p. 7681–7703 (2016).
39. W.C. Hammond, G. Blewitt, C. Kreemer and R.S. Nerem, *GPS Imaging of Global Vertical Land Motion for Studies of Sea Level Rise*, Journal of Geophysical Research: Solid Earth, **126** (2021).
40. L. Spilcă, *Learn what you need and learn it well*, MEAP Publication in October 2021 (estimated) ISBN 9781617298691, (2020).
41. J. Wilken, *Angular in Action*, ISBN 9781617293313, (2018).
42. H. Rocha, *Learn Chart.js*, Publisher(s): Packt Publishing ISBN: 9781789342482, (2019).
43. E. Nastase, A. Muntean, C. Ionescu, V. Mocanu and B.A.C. Ambrosius, *A regional GPS network for monitoring the Carpathian-Danubian-Pontic space deformations and the impact of local earthquakes*, Proceeding paper SGEM Conference III, 381–388 (2016).
44. E. Nastase, C. Oikonomou, D. Toma-Danila, H. Haralambous, A. Muntean and I.A. Moldovan, *Investigation of ionospheric precursors of earthquakes in Romania using the Romanian GNSS/GPS networks*, Rom. J. Phys. **61**, 1426–1436 (2016).